

# Chapter 1

## Problems with Light Emitting Devices and Their Solutions

This book reviews how to use an indirect transition-type semiconductor to construct light emitting diodes (LEDs) and lasers, which has not been possible with conventional methods employed in materials science and technology. First, this chapter surveys the problems to be solved. Some strategies and principles achieve solutions are reviewed. Detailed discussions of the theoretical aspects are described in Appendices A–E.

### 1.1 Introduction

The wavelength of the light emitted from a conventional LED is governed by the bandgap energy  $E_g$  of the semiconductor material used. Although there is a Stokes wavelength shift [1], its magnitude is negligibly small. Therefore, the value of  $E_g$  must be adjusted for the desired light emission wavelength, and this has been achieved by exploring novel semiconductor materials. For this purpose, direct transition-type semiconductors have been used for conventional LEDs. Among these semiconductors, InGaAsP has been used for optical fiber communication systems because the wavelength of the emitted light is 1.00–1.70  $\mu\text{m}$  ( $E_g = 0.73$ – $1.24$  eV) [2, 3]. When fabricating a highly efficient infrared LED or laser using InGaAsP, it is necessary to use a double heterostructure composed of an InGaAsP active layer and an InP carrier confinement layer. However, there are some problems with this approach, including the complexity of the structure and the high toxicity of As [4]. In addition, In is a rare metal. On the other hand, composite semiconductors that emit visible light, such as AlGaInP and InGaN, have extremely low emission efficiencies around the wavelength of 550 nm ( $=2.25$  eV) [5], which is called the green gap problem. Although this efficiency has been increasing recently due to improvements in dopant materials and fabrication methods, there are still several technical problems because highly toxic or rare materials are required, which increases the cost of fabrication.

In order to solve the problems described above, several methods using silicon (Si) have been recently proposed. Although Si has been popularly used for

electronic devices, there is a long-held belief in materials science and technology that Si is not suitable for use in LEDs and lasers because it is an indirect transition-type semiconductor, and thus, its light emitting efficiency is very low. The reason for this is that electrons have to transition from the conduction band to the valence band to spontaneously emit light by electron–hole recombination. However, in the case of an indirect transition-type semiconductor, the momentum (wave-number) of the electron at the bottom of the conduction band and that of the hole at the top of the valence band are different from each other. Therefore, for electron–hole recombination, a phonon is required in the process to satisfy the momentum conservation law. In other words, electron–phonon interaction is required. However, the probability of this interaction is low, resulting in a low interband transition probability.

In order to solve this problem, for example, porous Si [6], a super-lattice structure of Si and SiO<sub>2</sub> [7, 8], and Si nanoprecipitates in SiO<sub>2</sub> [9] have been used to emit visible light. To emit infrared light, Er-doped Si [10] and Si-Ge [11] have been employed. In these examples, the emission efficiency is very low since Si still works as an indirect transition-type semiconductor in these materials.

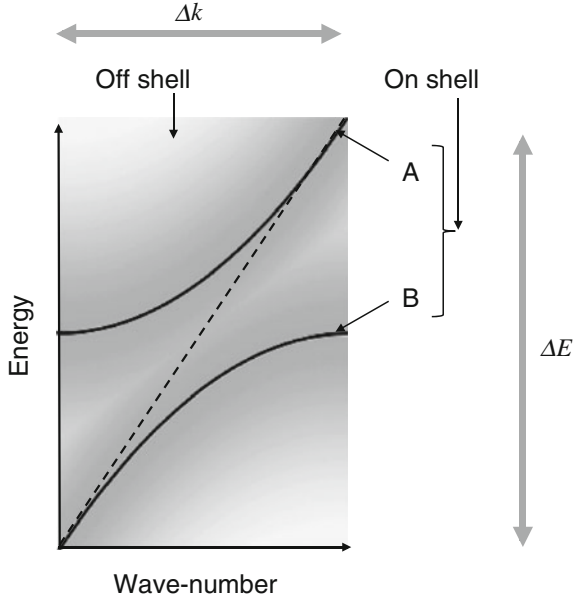
In contrast to these examples, as explained in this article, the use of dressed photons (DPs) and dressed-photon–phonons (DPPs) can realize highly efficient LEDs and lasers even when using Si bulk crystal.

## 1.2 Dressed Photons and Dressed-Photon–Phonons

First, as an introductory topic, the concept of elementary excitations is reviewed. Elementary excitations have been discussed for a long time in the field of solid state physics [12]. Excited states of a many-body system are regarded as a collection of certain fundamental excited states that has been called an elementary excitation, and also a quasi-particle. A phonon is a well-known example of a quasi-particle that represents the normal mode of crystal lattice vibration in a solid. Another example is a plasmon, which corresponds to the collective motion of electron density variations in an interacting electron gas. An exciton, another well-known example, represents a quasi-particle related to an electron–hole pair in a solid. The interaction between a photon and an exciton forms a new steady-state that also represents a quasi-particle called an exciton-polariton. Its dispersion relation, which is the relation between the wave-number  $k$  and energy  $E$  of the exciton–polaritons in macroscopic space, is represented by curves A and B in Fig. 1.1. It should be noted that the quasi-particles described above also follow dispersion relations that are similar to these curves.

Second, in preparation for starting the main topic of this section, it should be pointed out that there is a vast space around the curves A and B in this figure, which is represented by the gray shaded rectangle. A quasi-particle is also created in this space. By referring to the large size of this space, unique features of this quasi-particle are as follows:

**Fig. 1.1** Dispersion relation between the wave-number  $k$  and the energy  $E$ . The curves A and B represent the dispersion relation of the exciton-polariton. The broken line is that for light in free space. The gray shaded rectangle represents that for the dressed photons



- (1) As represented by the horizontal double-pointed gray arrow, the wave-number,  $k$ , of this quasi-particle spans a wide range. This also means that its uncertainty,  $\Delta k$ , is large, which represents the non-conservation of the quasi-particle’s momentum,  $\hbar k$  (where  $\hbar = h/2\pi$ , and  $h$  is Planck’s constant). This large uncertainty,  $\Delta k$ , also means that the quasi-particle is composed of a large number of normal modes. Furthermore, it means that the uncertainty,  $\Delta x$ , of the quasi-particle’s position,  $x$ , is small, due to Heisenberg uncertainty relation,  $\Delta(\hbar k) \cdot \Delta x \geq \hbar$ . This small uncertainty,  $\Delta x$ , means that the size of this quasi-particle is small.
- (2) As is represented by the vertical double-pointed gray arrow, the energy  $E$  of this quasi-particle spans a wide range. This means that its uncertainty,  $\Delta E$ , is large, which represents the non-conservation of the energy. The large uncertainty,  $\Delta E$ , also means that the time uncertainty,  $\Delta t$ , is small, due to Heisenberg uncertainty relation  $\Delta E \cdot \Delta t \geq \hbar$ . This means that this quasi-particle is created and subsequently annihilated within a short duration. In other words, the energy of this quasi-particle is temporally modulated, generating a large number of spectral sidebands.

The first feature, that is, the small size, means that the quasi-particle is created in a nanomaterial, and a part of the field of this quasi-particle penetrates through the surface of the nanomaterial to the outside. This penetrated field has been called the optical near field [13]. The second feature, the short duration, means that the quasi-particle is a virtual photon. A dressed photons (DP) provides a physical picture that describes these two features consistently, including the large number of normal modes and the spectral sideband features of (1) and (2), respectively.

For comparison, the exciton-polariton, represented by the curves A and B in Fig. 1.1, is a quasi-particle in a macroscopic material where the size of this material is much larger than the wavelength of light. This quasi-particle propagates toward the far-field and has been called a real photon; its momentum and energy are conserved ( $\Delta k = 0$ ,  $\Delta E = 0$ ). The behavior and properties of this real photon have been studied in conventional optical science and technology for a long time.

The curves A and B in Fig. 1.1 correspond to a physical system, which has been called “on shell” in quantum field theory [14–16]. On the other hand, the shaded gray rectangle has been called “off shell”. Whereas the real photon on shell conserves its momentum and energy, the virtual photon off shell does not. The probability of creating virtual photons diminishes depending on how far off shell they are. The value of this probability is represented by the gradation depth of the gray rectangle.

We now begin our discussion of the main topic, based on the first and second topics above. First, it is noted that the concept of a real photon on shell has been established in the conventional quantum theory of light [17]. The real photon corresponds to a quantum of the electromagnetic mode in a cavity defined in a macroscopic free space. Since the real photon is massless, it is difficult to express its wave function in a coordinate representation in order to draw a picture of the real photon as a spatially localized point-like particle, unlike an electron [18].

When describing the virtual photon off shell in a nanometric space, energy transfer between two nanomaterials and detection of the transferred energy are essential. They are formulated by assuming that the nanomaterials are arranged in close proximity to each other and illuminated by a real photon. Although the separation between the two nanomaterials is much shorter than the optical wavelength, it is sufficiently long to prevent electron tunneling. As a result, the energy is transferred not by a tunneled electron but by some sort of optical interactions between the two nanomaterials.

A serious problem, however, is that a cavity cannot be defined in a sub-wavelength-sized nanometric space, which differs from the approach taken in the conventional quantum theory of light. In order to solve this problem, an infinite number of electromagnetic modes and an infinite number of frequencies are assumed, corresponding to the large number of normal modes and spectral sidebands mentioned in (1) and (2) above, respectively. In parallel with this assumption, infinite numbers of energy levels must also be assumed in the electrons. Based on these assumptions, the dressed photons (DP) is defined as a virtual photon that dresses the electron energy (Appendix A) [19, 20]. The DP is modulated spatially and temporally due to features (1) and (2) above. The interaction between the two nanomaterials can be represented by energy transfer due to the annihilation of a DP from the first nanomaterial and its creation on the second nanomaterial.

Furthermore, since an actual nanometric system (composed of nanomaterials and DPs) is always surrounded by a macroscopic system (composed of macroscopic materials and real photons), energy transfer between the nanometric and macroscopic systems has to be considered when analyzing the interaction between the nanomaterials in the nanometric system. As a result, it is found that the magnitude of the transferred energy is represented by the Yukawa function (Appendix B). This analysis also elucidates an intrinsic feature of DPs, namely, the size-dependent

resonance; that is to say, the efficiency of the energy transfer between nanomaterials depends on the sizes of the nanomaterials that are interacting. It should be noted that this resonance is unrelated to diffraction of the real photon on shell, which governs the conventional wave-optical phenomena. Furthermore, since the DP is localized in nanometric space, the long-wavelength approximation, which is valid for conventional light–matter interactions, is not valid for DP-mediated interactions. As a result, an electric dipole-forbidden transition turns out to be allowed in the case of the DP-mediated interactions.

In actual materials, such as semiconductors, the contribution of the crystal lattice also needs to be included in the theoretical model of the DP. By doing so, it has been found that the DP interacts with phonons. Furthermore, in a nanomaterial, it is possible to generate multimode coherent phonons via a DP–phonon interaction. As a result of this interaction, a novel quasi-particle is generated. This quasi-particle is called a dressed-photon–phonon (DPP), which is a DP dressing the energy of the multimode coherent phonon (Appendix C). Furthermore, it is found that the DPP field is localized at the impurity sites in the crystal lattice of the nanomaterial with a spatial extent as short as the size of the impurity site. It is also localized at the end of the nanomaterial with a spatial extent as short as the size of this end.

The DPP energy can be transferred to the adjacent nanomaterial, where it induces a novel light–matter interaction. Here, since translational symmetry is broken due to the finite size of the nanomaterial, the momentum of the DPP has a large uncertainty and is non-conserved, as was the case of the DP itself. Also, since the DPP has an infinite number of spectral modulation sidebands as was the case of the DP, the electron dresses the energies of the photon and phonon, which means that the energy of the electron in the nanomaterial is also modulated.

When analyzing the conventional light scattering phenomenon in a macroscopic material, it has been sufficient to study one phonon. In contrast, the coherent phonon described above is composed of an infinite number of phonons. This coherent phonon assists in exciting the electron in the adjacent nanomaterial instead of merely increasing the material temperature, which enables DPP-assisted excitation of the electrons. Therefore, for analyzing the optical excitation of the nanomaterial, it is essential to represent the relevant quantum state of the nanomaterial by the direct product of the quantum states of the electron and the coherent phonon. This relevant quantum state means that an infinite number of energy levels has to be considered in the energy bandgap between the valence and conduction bands of an electron in the case of a semiconductor. This quasi-continuous energy distribution originates from the modulation of the eigenenergy of the electron as a result of the coupling between the DP and the coherent phonon. This DPP-assisted excitation and de-excitation can be exploited in the fabrication and operation of LEDs, lasers, and other devices using Si bulk crystals, which are reviewed in the following chapters.

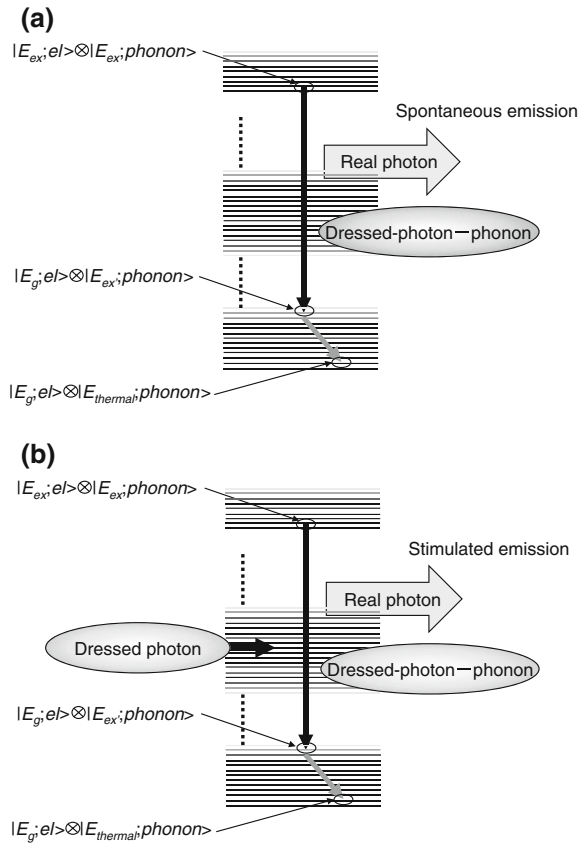
### 1.3 Principles of Photon Emission

For spontaneous emission of light by DPPs, a single-step or a two-step de-excitation of an electron takes place depending on whether the emitted real photon energy is higher or lower than the energy difference between the excited and ground states of the electron, which is  $E_g$  in the case of a semiconductor material (Appendix D). Stimulated emission also takes places in the same way.

#### 1.3.1 Single-Step De-Excitation

In Fig. 1.2a, b, since the electron strongly couples with the photon and phonon, the energy state is expressed as the direct product of the ket vectors of the electronic state and the phonon state. For example,  $|E_g; el\rangle \otimes |E_{ex}; phonon\rangle$  includes

**Fig. 1.2** Single-step photon emission processes via dressed-photon–phonon. **a** Spontaneous emission. **b** Stimulated emission



the ground state of the electron and the excited state of the phonon. The spontaneous emission of a DPP, as well as a real photon (Fig. 1.2a), is the result of the radiative transition from the excited state  $|E_{ex}; el\rangle \otimes |E_{ex}; phonon\rangle$  to the ground state  $|E_g; el\rangle \otimes |E_{ex'}; phonon\rangle$ . Here, in the case of a semiconductor, the excited and ground states of the electron, ( $|E_{ex}; el\rangle$  and  $|E_g; el\rangle$ ), correspond to the states in the conduction and valence bands, respectively. After the transition, the phonon in the excited state relaxes to the thermal equilibrium state ( $|E_{thermal}; phonon\rangle$ ) determined by the crystal lattice temperature, and finally the electron and phonon transition to the state  $|E_g; el\rangle \otimes |E_{thermal}; phonon\rangle$ .

The stimulated emission process (Fig. 1.2b) is explained as follows: When an electron in the excited state is irradiated with a DP, a transition from the initial state  $|E_{ex}; el\rangle \otimes |E_{ex}; phonon\rangle$  to the ground state  $|E_g; el\rangle \otimes |E_{ex'}; phonon\rangle$  takes place, resulting in photon emission. Like the spontaneous emission, the phonon then relaxes to a thermal equilibrium state determined by the crystal lattice temperature and finally the electron and phonon transition to the state  $|E_g; el\rangle \otimes |E_{thermal}; phonon\rangle$ .

### 1.3.2 Two-Step De-Excitation

Figure 1.3a schematically illustrates the two-step de-excitation for spontaneous emission (Appendix D).

**First step** The initial state is expressed by the direct product of the excited state of the electron and the excited state of the phonon, ( $|E_{ex}; el\rangle \otimes |E_{ex}; phonon\rangle$ ). De-excitation takes place from this initial state to the ground state  $|E_g; el\rangle$  of the electron. Since this de-excitation is an electric dipole-allowed transition, it generates not only a DPP but also a real photon. As a result, the system reaches the intermediate state  $|E_g; el\rangle \otimes |E_{ex'}; phonon\rangle$ . Here, the excited state  $|E_{ex'}; phonon\rangle$  of the phonon after DPP emission (route 1 in Fig. 1.3a) has a much higher eigenenergy than that of the thermal equilibrium state  $|E_{thermal}; phonon\rangle$ . This is because the DP couples with the phonon, resulting in phonon excitation. On the other hand, the excited state  $|E_{ex'}; phonon\rangle$  of the phonon after a real photon emission (route 2 in Fig. 1.3a) has an eigenenergy as low as that of  $|E_{thermal}; phonon\rangle$ . This is because the real photon does not couple with the phonon.

**Second step** This step is an electric dipole-forbidden transition because the electron stays in the ground state. Thus, only the DPP is generated by this emission process. As a result, the phonon is de-excited to the lower excited state  $|E_{ex''}; phonon\rangle$ , and the system is expressed as  $|E_g; el\rangle \otimes |E_{ex''}; phonon\rangle$ . After this transition, the phonon promptly relaxes to the thermal equilibrium state, and thus, the final state is expressed as  $|E_g; el\rangle \otimes |E_{thermal}; phonon\rangle$ . The de-excitation for the stimulated emission is explained by Fig. 1.3b, which is similar to Fig. 1.3a. The only difference is that the DP is incident on the electron in the excited state, triggering stimulated emission.

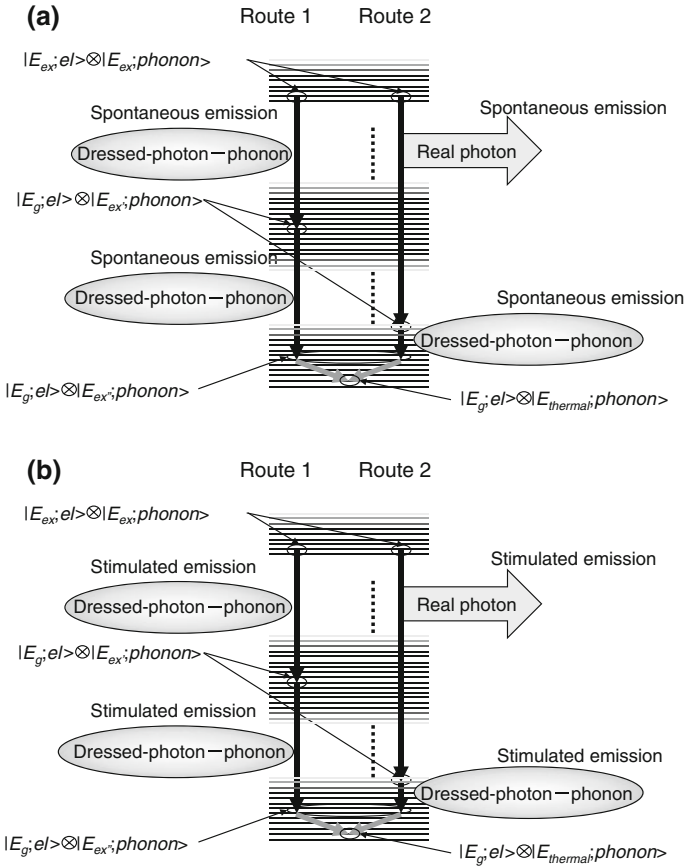


**Fig. 1.3** Two-step photon emission processes via dressed-photon-phonon. **a** Spontaneous emission. **b** Stimulated emission

### 1.4 Photon Breeding

The following chapters review novel LEDs and lasers fabricated by using Si crystals and other relevant indirect transition-type semiconductor crystals. Prior to this review, it should be pointed out that the fabrication and operation principles of these devices are different from those of conventional LEDs and lasers fabricated by using direct transition-type semiconductors. This section describes these differences.

To realize a device by using Si crystal, dressed-photon-phonons (DPPs) are used two times: first for device fabrication, and second for device operation.

- (1) For device fabrication, a p-n homojunction-structured Si crystal is annealed, via Joule-heat produced by current injection, in order to diffuse boron (B) atoms (the p-type dopant). During the annealing, the Si crystal surface is irradiated

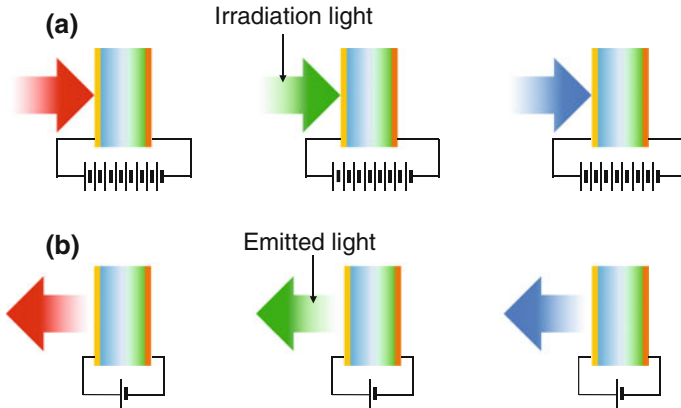


**Fig. 1.4** Light emitting devices using Si. **a** Fabrication. **b** Operation

with light (a real photon) (Fig. 1.4a) to create DPPs on the B atom surface. Driven by the created DPPs, electron–hole recombination takes place, emitting light (a real photon). Since the energy of the emitted light dissipates from the Si crystal, the efficiency of the Joule-heating decreases. As a result, a unique spatial distribution of B atoms is realized, which depends on the created DPP energy. This novel annealing is called DPP-assisted annealing. In this spatial distribution, neighboring B atoms form a pair, and the resultant B atom pair orients in a specific direction to efficiently create localized phonons (Sects. 3.3 and 4.3.3).

- (2) For the operation of the fabricated Si-LED, the light irradiation is not required any more; it is used only during the DPP-assisted annealing. Only forward current that is much lower than that used for annealing is injected, as is the case of the conventional LED operation. By this forward current, an electron is injected into the conduction band at the p–n homojunction and creates a photon by spontaneous emission even though its probability is very low. However, once this photon is created, it subsequently creates a DPP on the surface of the B atom at the p–n homojunction, and this DPP interacts with another electron in the conduction band to exchange momentum so that a secondary photon is created. By repeating these momentum exchange and photon creation processes, the emitted light intensity is amplified and reaches a stationary value within a short duration, so that light with a sufficiently high intensity is emitted from the p–n homojunction.

It should be noted that photon breeding occurs during device operation. As a result, the photon energy of the emitted light is equal to the photon energy  $h\nu_{anneal}$  of the light irradiated during the annealing (Fig. 1.4b). This is in contrast to a conventional device, where the photon energy of the emitted light is determined by  $E_g$ . This is because the difference between  $h\nu_{anneal}$  and  $E_g$  is compensated for by the energy of the created phonons. This means that the photon energy of the light

emitted from the device is identical to  $h\nu_{anneal}$ . This is because the spatial distribution of the B atoms has been controlled by the light irradiated during the DPP-assisted annealing, enabling most efficient stimulated emission and spontaneous emission of photons with identical photon energy. In other words, the light irradiated during the DPP-assisted annealing serves as a “breeder” that creates photons with an energy equivalent to  $h\nu_{anneal}$ . This is the reason why this novel phenomenon is named photon breeding with respect to photon energy. Photon breeding has been observed in the radiation energy dissipation process from relativistic jets in blazars [21, 22]. However, in this astrophysical phenomenon, a very-high-energy photon (X ray) is generated from a low-energy photon (infrared or visible light) by inverse Compton scattering with a charged particle. Therefore, the photon breeding discussed in this book, producing equal-energy photons by using a DPP in a nanometric-sized space in a material, is quite different from that described above. Due to this difference, the present photon breeding may have to be called “nano-photon breeding” in order to avoid confusion. However, this book uses the name “photon breeding” for conciseness.

Photon breeding has been observed not only for the photon energy but also for the photon spin (Sects. 3.4 and 6.3). For example, linearly polarized light is emitted from the LED if it was fabricated by irradiating linearly polarized light during the annealing step. (Remember that the light emitted from a conventional LED is not polarized.)

In summary, the principles, operation, and functions of the present devices are different from those of conventional LEDs and lasers because DPPs and electric dipole-forbidden transitions are involved. Furthermore, photon breeding occurs, so that the energy and spin of the emitted photons are identical to those of the light irradiated during the annealing. Due to this difference, it is appropriate to call this novel device “a third light source”, or more concretely, “a photon breeding device”.

## 1.5 Fabrication and Performance of Photon Breeding Devices

As the last topic of Chap. 1, this section summarizes the fabrication and performance of the photon breeding devices that will be reviewed in the following chapters.

### 1.5.1 Fabrication

(1.1) In DPP-assisted annealing, an electric current is injected into the sample while irradiating it with light (photon energy:  $h\nu_{anneal}$ ). (Refer to Sects. 2.2 and 3.1.)

(1.2) DPP-assisted annealing is possible even when the value of  $h\nu_{anneal}$  is lower than  $E_g$  (Refer to Sect. 3.1.)

- (1.3) The optimum condition for effective DPP-assisted annealing is that the ratio of the electron injection rate to the photon irradiation rate be set to 1:1. (Refer to Sect. 7.1.)
- (1.4) The sample's temperature during the DPP-assisted annealing can be as low as 400 K; in other words, an extremely high temperature is not required. (Refer to Sects. 2.2, 3.1, and 7.1.)
- (1.5) Conventional thermal annealing, e.g., by heating the sample in an electric furnace, is not compatible with the fabrication of photon breeding devices. (Refer to Sect. 7.1.3.)

### 1.5.2 *Spatial Distribution of the Dopant Atoms*

- (2.1) As a result of DPP-assisted annealing, p-type dopant atoms (B atoms in the case of a Si crystal) form pairs. The separation,  $d$ , between the dopant atoms in the pair is given by  $d = na$ , where  $a$  is the lattice constant of the crystal. The integer  $n$  satisfies the relation  $h\nu_{anneal} = E_g - nE_{phonon}$ , where  $E_{phonon}$  is the energy of the created phonon. (Refer to Sect. 3.3).
- (2.2) The orientation of the pair of the dopant atoms is perpendicular to the propagation direction of the light irradiated during the DPP-assisted annealing. Furthermore, in the case where this light is linearly polarized, it is also perpendicular to the direction of polarization. (Refer to Sect. 3.4.)

### 1.5.3 *Performance*

- (3.1) The fabricated devices exhibit electroluminescence by injecting an electric current. (Refer to Sects. 2.2 and 3.1.)
- (3.2) The photon energy of the emitted light is identical to  $h\nu_{anneal}$ ; i.e., photon breeding takes place with respect to the photon energy. (Refer to Sects. 2.2 and 3.1.)
- (3.3) The polarization direction of the emitted light is identical to that of the light irradiated during the DPP-assisted annealing; i.e., the device exhibits photon breeding with respect to the photon spin. (Refer to Sects. 3.4 and 6.3.)
- (3.4) When the device is fabricated under the condition described in (1.2) above, the photon energy of the emitted light is lower than  $E_g$ , as can be deduced from (3.2). Therefore, the emitted light is not absorbed by the crystal, enabling high efficiency and high output power. (Refer to Sects. 3.2, 5.3, 6.1–6.4, 7.1, and 7.2.)

**Table 1.1** Family of photon breeding devices

Devices	Photon energy	Crystal	Chapters and sections to refer to
Light emitting diode	Visible	Si	Chap. 2
		SiC	Chap. 6
		GaP	Sect. 7.1
		ZnO <sup>1</sup>	Sect. 7.2
	Infrared	Si	Chap. 3
Laser	Infrared	Si	Chap. 5
Optical and electrical relaxation oscillator	Infrared	Si	Sect. 8.1
Photodiode <sup>2</sup>	Infrared	Si	Sect. 8.2
	Visible	Si	Sect. 8.2
Modulator <sup>3</sup>	Visible	ZnO <sup>1</sup>	Sect. 8.3
		SiC	Sect. 8.3

<sup>1</sup>Although ZnO is a direct transition-type semiconductor, a p-type semiconductor is difficult to fabricate by the conventional method

<sup>2</sup>Provided with optical amplification gain

<sup>3</sup>Light polarization rotator and light beam deflector

### 1.5.4 Family of Photon Breeding Devices

The photon breeding devices that have been fabricated are listed in Table 1.1.

## References

1. F. Yang, M. Wilkinson, E.J. Austin, K.P. O' Donnell, Phys. Rev. Lett. **70**, 323 (1993)
2. ZhI Alferov, Semiconductors **32**, 1 (1988)
3. R.A. Milano, P.D. Dapkus, G.E. Stillman, I.E.E.E. Tran, Electron Devices **29**, 266 (1982)
4. U.S. Department of Health and Human Services, Public Health Service, National Inst. Health, National toxicology program (ed.), *NTP Technical Report on the Toxicology and Carcinogenesis Studies of Indium Phosphide* (U.S. Department of Health and Human Services, Washington, DC., 2012) NTP TR 499
5. K.T. Delaney, P. Rinke, C.G. Van de Walle, Appl. Phys. Lett. **94**, 191109 (2009)
6. K.D. Hirschman, L. Tysbekov, S.P. Dutttagupta, P.M. Fauchet, Nature **384**, 338 (1996)
7. Z.H. Lu, D.J. Lockwood, J.-M. Baribeau, Nature **378**, 258 (1995)
8. L. Dal Negro, R. Li, J. Wurga, S.N. Beasu, Appl. Phys. Lett. **92**, 181105 (2008)
9. T. Komoda, Nucl. Instrum. Methods Phys. Res. Sect.B, Beam Interact. Mater. Atoms **96**, 387 (1995)
10. S. Yerci, R. Li, L. Dal Negro, Appl. Phys. Lett. **97**, 081109 (2010)
11. S.K. Ray, S. Das, R.K. Singha, S. Manna, A. Dhar, Nanoscale Res. Lett. **6**, 224 (2011)
12. D. Pines, *Elementary Excitation in Solids* (Perseus Books, Reading, 1999)
13. M. Ohtsu, K. Kobayashi, *Optical Near Fields* (Perseus Books, Reading, Massachusetts, 1999) (Springer, Berlin, 2004)
14. M. Thomson, *Modern Particle Physics* (Cambridge University Press, Cambridge, 2013)

15. R.P. Feynman, *The Theory of Fundamental Processes* (W.A. Benjamin, New York, 1962), pp. 95–100
16. M. Ohtsu, H. Hori, *Near-Field Nano-Optics* (Kluwer Academic/Plenum Publishers, New York, 1999), pp. 29–31
17. J.J. Sakurai, *Advanced Quantum Mechanics* (Addison-Wesley, Reading, 1967)
18. T.D. Newton, E.P. Wigner, *Rev. Mod. Phys.* **21**, 400 (1949)
19. M. Ohtsu, *Progress in Nanophotonics 1*, ed. by M. Ohtsu (Springer, Berlin, 2011), pp. 1–4
20. M. Ohtsu, *Dressed Photon* (Springer, Berlin, 2013), pp. 11–18
21. J. Poutanen, B.E. Stern, *Mon. Not. R. Astron. Soc.* **372**, 1217 (2006)
22. B.E. Stern, J. Poutanen, *Mon. Not. R. Astron. Soc.* **383**, 1695 (2008)



<http://www.springer.com/978-3-319-42012-7>

Silicon Light-Emitting Diodes and Lasers  
Photon Breeding Devices using Dressed Photons

Ohtsu, M.

2016, IX, 192 p. 135 illus., 38 illus. in color., Hardcover

ISBN: 978-3-319-42012-7